Review Article: Variable Optical Elements for Fast Focus Control

SeungYeon Kang[1,3], Martí Duocastella[2,4], and Craig B. Arnold[1,*]
[1] Department of Mechanical and Aerospace Engineering, Princeton University, New Jersey, 08540
[2] Nanophysics, Isituto Italiano di Tecnologia, 16163 Genova, Italy
[3] Current: Mechanical Engineering, University of Connecticut, Storrs, Connecticut, 06269
[4] Current: Department of Applied Physics, Universitat de Barcelona, 08028 Barcelona, Spain
* Corresponding author. Email: cbarnold@princeton.edu

Abstract

In this article, we survey recent developments in the emerging field of high-speed variable z-focus optical elements, which are driving important innovations in advanced imaging and materials processing applications. 3D biomedical imaging, high-throughput industrial inspection, advanced spectroscopies, and other optical characterization and materials modifications methods have made great strides forward in recent years due to precise and fast axial control of light. Three state-of-the-art key optical technologies that enable fast z-focus modulation are reviewed along with a discussion on the implications of what the new variable optical element developments entail and the resulting impact on technologically relevant applications.

Technological advances that increase the speed and precision of light-focus control have enabled new opportunities in imaging and materials processing applications. Previously, the goals of obtaining fundamental understanding of sub-cellular dynamics and achieving highly efficient laser processing methods have been stifled by slower optics that inevitably come hand in hand with excessive light-exposure on photosensitive living organisms and slow acquisition of light information. The key to resolving these problems is to modulate focus of light at very high-speeds in all three dimensions which minimizes prolonged light-exposure on living organisms and increases light-based-information acquisition-rate, leading to innovations that have not been possible with slower systems. Recent achievements such as video-rate optical microscopy of sub-cellular dynamics, increased throughput in laser micromachining, and spectroscopic determination of physical parameters are advancing various areas including 3D biomedical imaging, industrial manufacturing and advanced spectroscopies. Therefore, it is invaluable for both scientific and industrial communities to look into the state-of-the-art optical technologies that enabled the advancements and their implications for future applications.

The central question in the design of any tunable optical system is how fast one can control the focal position of light across the three dimensions of space. For imaging applications, light-focus control can determine the rate at which three-dimensional (3D) information can be retrieved from a sample – the understanding of key processes such as neuronal signaling or molecular diffusion depends on it. In laser materials processing, fabrication throughput is directly correlated to the speed at which one or multiple laser foci can be moved across a workpiece. While fast control of light along the x- and y-direction is straightforward to implement using mirrors or light deflectors, a classical problem in optics has been to attain the same degree of control along the z-direction. Indeed, traditional methods based on mechanically moving the sample or optical components impose serious speed restrictions in z-focus

translation – up to three orders of magnitude slower than along the x- and y- direction. Therefore, modern technologies focus on compensating such speed imbalance by developing remote-focusing systems with higher z-focusing speed. Box 1 explains how the remote-focusing variable optical systems use changes in optical power to achieve z-focus control.

In this review we focus on the development in the speed of the variable optical elements which opened the doors to exciting advanced applications. We use the term high-speed to refer to variable optical elements with a focus-varying response time that is faster than a millisecond (ms), and we use the term ultra-high-speed to narrow variable optical elements down to those with a response time of a microsecond (µs) and faster. Extra attention is given to recent ultra-high-speed variable optics that allowed reaching a µs response time. Phenomena relevant to the µs time scale includes the triplet state relaxation of fluorophores, the typical pixel dwell time of a point scanning microscope and heat dissipation. Therefore, controlling light at these speeds enables novel light-matter interactions that would not be possible with slower systems such as reduced photobleaching, fast 3D particle tracking or enhanced laser processing. The review is divided into 3 sections. In the first section of the review, we analyze and present the key technologies in variable optical elements that allowed to achieve sub-ms and µs response time. Next, we review the new implications the development in ultra-high-speed variable focusing entails and discuss the resulting impact on technologically relevant areas. We conclude with a discussion of the future outlook on variable optical elements for important innovations in advanced imaging and materials processing applications.

Box 1. Axial focus tuning with variable optical elements

The focal length of a varifocal lens (VL) can be generally written as $f_{VL}\ (x)$, where x represents the lens operating signal. The mathematical expression of $f_{VL}\ (x)$ depends on the particular working principle of the lens, but the attainable change in optical power (ΔOP) is always given by:

$$\Delta OP = \frac{1}{f_{VL}(x_1)} - \frac{1}{f_{VL}(x_2)}$$

where $f_{VL}(x_1)$and $f_{VL}(x_2)$ correspond to the respective minimum and maximum focal length values. When using a VL as the last optical element for light focusing or for imaging, the axial focus position directly corresponds to the focal length or it can be easily calculated using paraxial optics (Box figure a). However, most VL systems have a low numerical aperture (NA) and thus to gain spatial resolution, they are usually combined with high NA focusing optics. In this case, the optimal position of the VL that avoids magnification effects, preserves resolution and maximizes the axial scan range corresponds to a conjugate plane of the rear focal plane of the focusing lens (Box figure b). By using geometrical optics, the displacement in z-focus position $z(x)$ with respect to the native focusing plane of a lens with focal length f_0 can be calculated as[103]:

$$z(x) = \frac{-{f_0}^2}{{M_R}^2 f_{VL}(x)}$$

where M_R is the magnification factor of the relay lens system and the total scan range Δz is:

$$\Delta z = -{f_0}^2 \Delta OP / {M_R}^2$$

There are several important factors to consider when choosing the appropriate VL for a given application. Besides the change in optical power, the physical aperture of the varifocal system plays a key role. For example, to match the aperture of the focusing lens and exploit its full NA, a relay lens system with a magnification above 1 may be needed, which can reduce Δz. Importantly, the axial focus shift induced by a VL can result in spherical aberration. In particular, the defocus term at a distance z' with respect to the native focusing plane can be described by a phase term[44,104]:

$$\varphi \approx kz' - \frac{1}{2}\rho^2 kz' \sin^2\alpha - \frac{1}{8}\rho^4 kz' \sin^4\alpha$$

where k is the wavenumber, ρ is the normalized pupil radius, and α is the maximum acceptance angle of the lens, determined from its NA. Although the first phase term can be typically ignored and the second term can be cancelled with a VL, the residual aberration corresponding to the third term can only be compensated by adaptive optics. Therefore, for high NA systems or when moving the focus far away from their native focusing plane, extra caution is required to limit the undesirable effects.

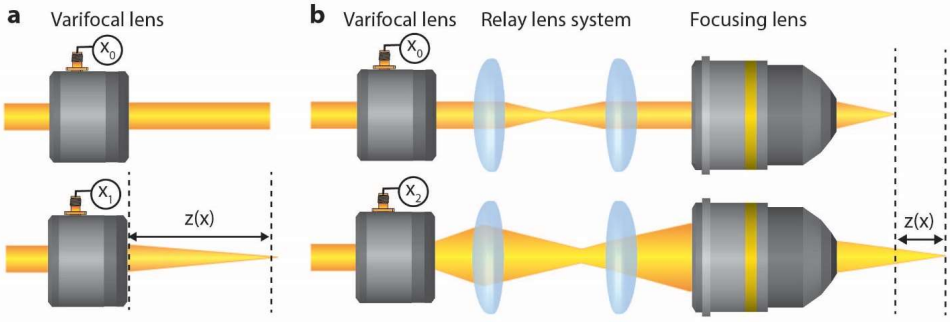

Box figure. Strategies for axial focus control using a variable optical element. a) Focusing with the varifocal lens as the last focusing element. b) Normal configuration for high-resolution imaging or tight focusing. The varifocal lens is placed at a conjugate plane of the high NA focusing lens.

The key enabling technologies for shifting towards higher-speed variable focus

In order to determine the key technologies that enabled higher-speed variable focusing, we performed a meta-analysis on a comprehensive set of variable-optic-element studies and summarized it in Table 1 and Figure 1(a). Table 1 categorizes the various types of varifocal optical systems based on their material components and working principles and figure 1 shows the speed of the varifocal optical systems categorized in table 1 in terms of response time. By categorizing varifocal optical systems based on their material components and working principles, we identify that the development of higher-speed varifocal optics has been carried out in two directions; one by improving the material response-time and the other by applying faster working principles. For example, the slow response time for mechanical-wetting lenses has been improved by adopting new fast-response materials such as ferroelectric liquid crystals or by implementing elements such as adaptive optics or acoustic waves that can drive the varifocal optics at a faster rate.

Type / Working Principle		Material / Components		Tuning power [1/m]	Aperture or Beam diameter
Mechanical lens		Alvarez lens[1–3] & Moiré lens[4] : Two patterned refractive lenses or diffractive elements are translated or rotated relative to each other		-50 to 50	1 -10 mm
Electronic liquid/ polymer lens	Membrane or liquid shape deformation[5] (Electro-mechanical)	Membrane -structured	Glass diaphragm or elastic membrane with microfluidic channels and fluidic actuation[6–10]	0 to 200	100 µm - 100 mm
			Meta-lens[11–13] : Metasurface optics and dielectric elastomer actuators	15 to 7000	10 µm - 10 mm
		Membrane -less	Dielectric lens : Dielectric liquid with high voltage source [14–16]	20 to 2000	100 µm - 10 mm
			Electro-wetting lens : Conducting liquid with high voltage source[17–21]	-500 to 1500	100 µm - 10 mm
			Mechanical-wetting lens : Immiscible liquids and sharp interface with microfluidics - Ferrofluidic actuator [22,23] - Piezoelectric transducer[24] - Manual actuation[25] - Hydrogel lens[26] :	-500 to 50	1 - 10 mm
	Refractive index gradients	Electro-optical liquid crystal (LC) lens [27–32]		0 to 2000	100 µm - 30 mm
Electro-optic ceramic lens		Potassium tantalate niobate (KTN) lens [33–35]		0 to 2.5	1 – 10 mm
		Lead–lanthanum zirconate–titanate (PLZT) lens [36]		0 to 10	1 – 10 mm
Acoustic lens		Tunable Acoustic Gradient index (TAG) lens: : Acoustic wave generated by a piezoelectric material[37–39]		-30 to 30	~ 10 mm
Acousto-optic system	Bragg diffraction	Acoustic optic deflector (AOD) system[40,41]: : Two acousto optic modulators (AOM) driven with a chirped frequency		-2 to 2	1 – 10 mm

Other adaptive-optical element (AOE) systems	- Multi-plane light conversion device[42] - Deformable mirrors (DM) & spatial light modulators (SLM)[1,43–45]	-0.5 to 0.5, but depends on the stroke excursion or of DM bit depth of SLM	100 µm - 10 mm

Table 1. Classification of varifocal optical systems based on working principles. Tuning power and beam size values are extracted from review papers and references in the table.

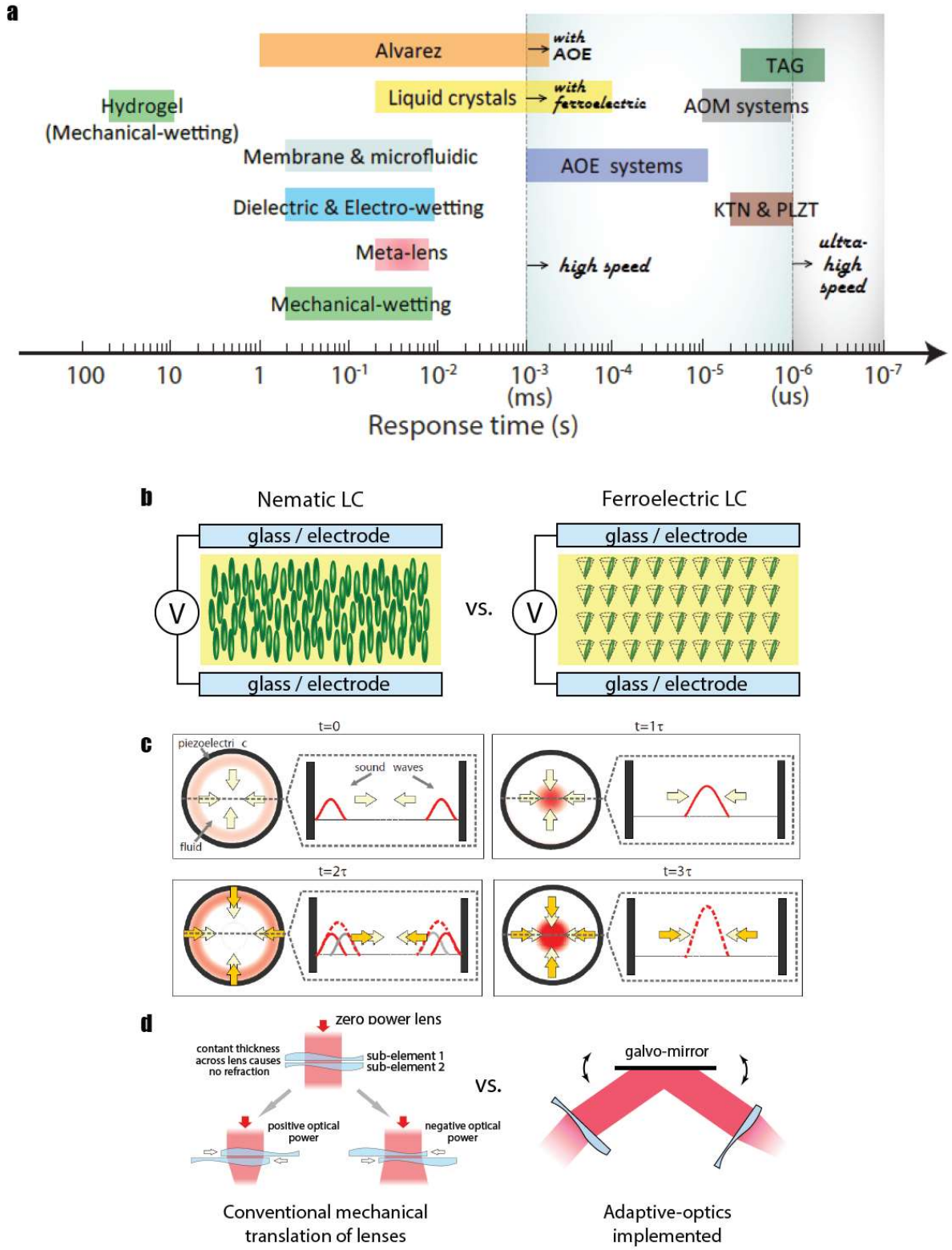

Figure 1. Performance of varifocal optical systems and the key three higher focal-varying speed enabling technologies. *(a) Response time of varifocal optical systems from data gathered in Table 1. Dashed lines represent definition of high-speed and ultra-high speed, (b) Nematic phase LCs with randomly positioned center of mass and long-range directional order vs.*

Smectic C phase FLCs with well-defined layers and chirality (often shown with a cone to show the director tilt of each layer), (c) Scheme of the acoustically driven fluid lens model with TAG lens as a resonator. Cylindrical acoustic waves travel back and forth in the TAG lens, interfering with each other and producing periodic changes in the lens optical power every 2 τ. From ref [46], (d) Schematic of modified Alvarez lens via beam steering using adaptive optics. Image modified from ref[1].*

Here, we introduce three recent technologies that enabled development of higher-speed varifocal optics, either by improving the material response-time or through implementation of faster driving methods. Ferroelectric liquid crystal lenses and adaptive optical technologies have enabled sub-ms response times and high-speed acoustic waves have been used to allow unique innovations in the µs response time. Due to the ultra-fast speed capabilities, new scanning microscopy applications are enabled that work at the µs time scale such as for triplet-state relaxation and also at the tens of µs- time scale for typical pixel dwell times. Elaborate time dependent behavior characterization studies such as determination of molecular diffusion coefficients in free solution have become possible, and the ability to micromachine on the µs time scale has brought higher efficiency in laser-processing applications. Note that even though electro-optic ceramic lenses such as KTN & PLZT operate at near ultra-high speeds, due to their long history of development we focus more on the recent developments that include use of ferroelectric liquid crystals, acoustic waves and adaptive optics.

Ferroelectric liquid crystal lens. Liquid crystal (LC) lenses offer tunable refractive indices from varying LC orientations based on the optical and dielectric anisotropies in response to an electric field. Changes in focal length are then obtained by using LC with a curved surface or, alternatively, by applying an axially symmetric non-uniform electric field with patterned electrodes. While several types of LCs structures exist, lenses have conventionally been implemented with those exhibiting a nematic phase, featuring rod-like molecules arranged in random positions while maintaining a long-range order (figure 1b). Despite the long history of development in LC lenses, the intrinsic highly oriented nematic phase properties result in a slow response time in the order of a few 10s-100s of ms[47]. More information on the conventional LC lenses can be found in other review articles[29,47,48]. Reduction in the dimension and addition of functionalized polymers have been attempted to achieve faster response time with nematic LCs but are yet unable to reach sub-ms[49]. Lenses with a relatively fast response time can be obtained by using LCs with a highly twisted chiral nematic phase. The higher speed appears when operated at a specific temperature range near the LC–isotropic transition point, where the so-called blue phases appear. In this case, though, the restricted temperature working range[50] limits practical implementation and recent efforts in trying to increase it are being made through the addition of polymer or surface-functionalized nanoparticles[51].

What allowed the development of high-speed LC varifocal optics was the implementation of ferroelectric LCs with a smectic C* (* represents chirality) phase. They present well-defined layers and chirality which leads to a spontaneous polarization response to an electric field that allows sub-ms optical switching time[52] (figure 2a). Although the basic principles of ferroelectric LCs have been around since 1980, much development has been made recently with the large display market growth in consumer electronics. New crystal structures and methods to further amplify the spontaneous polarization response of ferroelectric LCs to increase the speed are being investigated[53–55]. Ferroelectric LCs capability to fast

phase modulate has been opening doors to new exciting applications in LC photonic devices such as photobiomodulation in light-therapy or LC on silicon technology[56,57].

Acoustically driven fluid lenses. A tunable acoustic gradient index (TAG) lens, also referred to as an ultrasound lens, uses acoustic waves generated by a piezoelectric material to radially excite a refractive fluid-filled cylindrical cavity with two flat glass windows and induce ultra-high-speed variation in focal-length[37–39]. As shown in figure 1c, the stronger radial vibration modes of the cylindrical piezoelectric generate waves at the wall with a driving frequency (t=0). At t=τ, the first set of waves travel to the center of the lens. At t=2τ, the waves travel back to the cylindrical wall and interferes with a new set of waves generated. The combined waves travel back to the center at t=3 τ, resulting in a variation in the amplitude with a periodicity of 2τ. The waves continuously travel back and forth interfering with each other to reach steady state. It is these standing wave density oscillations within the refractive fluid that result in a continuously scanning gradient index of refraction and corresponding variable focal length. By driving the lens with a sound wave at the lens' resonance frequency, it allows a single axial scan to achieve unsurpassed speeds of a μs or less. The ability of the acoustic driven fluid lenses to rapidly modulate the focus can be combined with two-photon point scanning microscopy or fluorescence correlation spectroscopy or light-sheet microscopy techniques to image three-dimensionally continuously moving biological systems with various velocities and accelerations[58–60], to enhance 3D resolution in optical coherence tomography[61],to determine molecular diffusion coefficients of proteins in living organisms by estimating the change in the size of the encapsulated volume[62], and in industrial applications to provide increased efficiency in micromachining and inspection analysis rate[63–65].

Enhanced adaptive optical technologies. Another way to achieve faster varifocal response time is to make use of galvano mirrors or adaptive optical elements (AOEs) such as deformable mirrors (DMs) and spatial light modulators (SLMs) that intrinsically perform at high-speeds. In these cases, the optical power of non-imaging elements capable of wave front modulation is often evaluated by the extended depth of field (DOF) in contrast to the optical power of the lens or numerical aperture. Alvarez lens is one example that has been invented in the late sixties and has recently been modified by combining the advantages of multiple optical elements to achieve varying focal capabilities at high speeds[1]. Alvarez lens is composed of two refractive lenses each with a plano surface and a cubic profile surface that are placed in inverse and translated with respect to each other to adjust the focus. Multiple sub-elements or Alvarez lens pairs are also used to further extend the focus[3]. In contrast to the classical mechanical translation approach, Bawart et al. placed a galvo-mirror in between the two lenses to acquire change in optical power through beam deflection rather than from displacement of the lenses[1]. By using galvo-mirror that already performs in the sub-ms, they were able to shift the response time of conventional Alvarez lenses into the high-speed regime (figure 1d). Other examples of using enhanced adaptive optical technologies include works by Booth et al.[44,45] and Mertz et al.[43] where they used AOEs to create extended DOF for volumetric imaging. In these examples, AOEs are positioned so that the phase of incident wave-fronts get altered at high speeds either to displace focal spot or to achieve extended DOF.

It is worthwhile to note that all ultrahigh speed variable optics have limitations that should be considered when applying them. For instance, variable optical elements which operate through

transmission in a refractive fluid or fluid-like medium have a tendency to exhibit absorption at high optical power leading to potential thermal lensing or other heat-related phenomena[14,50,66,67]. Similarly, those with low NA elements are less effective as stand-alone lenses and typically must be coupled to high NA objectives that are corrected for large field imaging which can lead to spherical aberration as described in Box 1. More specifically to each system, ultrasound driven lenses are limited to fast sinusoidal scanning[44] and LC lenses are limited to small dimensions to minimize disruption in the alignment of LCs[29,48]. Even though AOE systems have the advantage of compensating for aberrations, they are typically complex and require precise alignment with actual lens components[42,45]. Thus, their performance varies vastly depending on the setup.

Implications of the ultra-high-speed variable focus optics in important applications

The recent high-speed and ultra-high-speed varifocal enabling technologies discussed previously imply that exciting innovations can be made in various applications for both science and industry community. Examples on advancements in high-speed and ultra-high-speed applications in technologically relevant areas such as volumetric imaging, microscopy, single particle tracking and laser processing are presented.

Reduced photobleaching and phototoxicity. The exposure of living cells or organisms to light can have damaging effects to their health, a phenomenon generally known as phototoxicity. Phototoxicity is typically aggravated in live imaging and spectroscopy techniques that use samples labeled with fluorophores or other fluorescent probes[68]. In this case, fluorescence excitation produces damaging free radicals, which can alter cell function or even induce cell death if generated at rates above the tolerance levels that cells naturally possess. Importantly, because the fluorescence quantum yield of common dyes or proteins is typically low, to maintain a strong fluorescence flux relatively high excitation intensities are used which further increase the risk of photon-induced damage. Intense excitation can also result in photobleaching, namely the progressive loss of fluorescent signal. While phototoxic effects can be obviated in fluid mechanics or polymer sciences with inert fluorescent-labeled samples, photobleaching is the other obstacle that can perturb or even impede the collection of the signal of interest.

Fast axial focus control of light is a promising solution for preventing the critical concern of photobleaching and phototoxicity[69]. Figure 2 shows the two main pathways that can lead to reduced photon-induced damage with ultra-high-speed variable focus systems. Both pathways make use of fast splitting of the light focus into an arbitrary number of sections along the optical axis, as illustrated in Figure 2a. The first pathway gives advantage of focus splitting for potential reduction in the total amount of excitation power delivered to the sample and, consequently, of the photo-toxic or photo-degradation effects. For example in light-sheet microscopy[70], implementation of varifocal optics enables confinement of illumination to a user-defined number of *4D (x,y,z,time)* regions of interest (ROI) as shown in figure 2b. Because the rest of the sample remains unexposed, volumetric imaging using varifocal optics results in a significant reduction of the total light dose. In addition, the increase in the number of sections interrogated can lead to improved statistics and facilitates low excitation intensities as shown in figure 2c. This has been successfully proved in fluorescence correlation spectroscopy (FCS) applications where the use of a varifocal lens allowed collecting of accurate correlation curves over shorter times and hence at lower light doses than standard FCS[62]. The second pathway demonstrates the benefit of fast focus splitting

by modulation of illumination (figure 2d). The axial displacement of the focus generated with varifocal optics allow each axial section to be discontinuously illuminated, with a period that can be in the microsecond time scale. Notably, periods of darkness have been found to play a major role in reducing photobleaching[71]. One of the main causes of photobleaching is the excitation of molecules from the triplet state (T_n), which has a normal relaxation time of microseconds as shown in figure 2e. By using inter-pulse dark periods during illumination modulation, the excited molecules can relax back to the ground state and diminish the probability of photobleaching. This process eliminates photodamage for studies such as recording of calcium dynamics in live neurons, even if the total excitation power applied was higher than for 2D imaging[59]. Similar results have been found when assessing photobleaching effects in two-photon[72] and light-sheet[60] microscopy, demonstrating the potential advantages of variable optical elements for the characterization of light-sensitive systems.

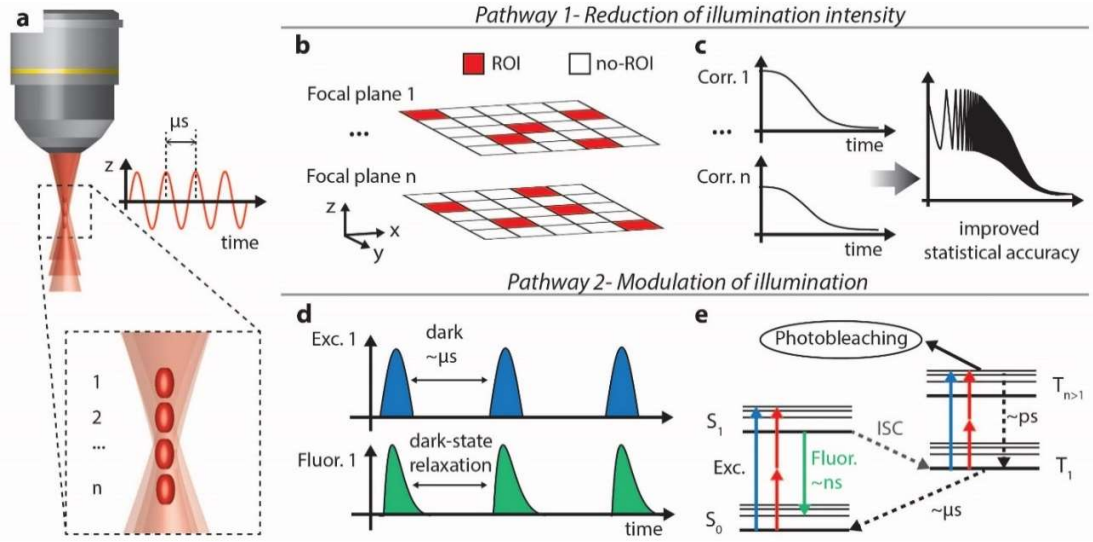

Figure 2. Pathways to limit photobleaching and phototoxicity using fast variable optical elements. *a) Schematic of the effects induced by fast axial scanning, allowing the splitting of the focus into several axial sections. b) Selection of tailored regions of interest (ROI) or c) improved statics in correlation (Corr.) techniques enable the reduction of the overall illumination of the sample and help prevent photodamage. d) The discontinuous excitation (Exc.) at microsecond time scales produced by fast axial scanning enables the relaxation of the triplet state typically responsible for photobleaching. e) Jablonsky diagram of a typical organic fluorophore, indicating the major molecular routes for excitation (Exc), fluorescence (Fluor.), intersystem crossing (ISC) and relaxation (dashed lines).*

Real-time volumetric imaging. Volumetric information from a sample is normally acquired through a sequence of images from different focal planes, the so-called z-stack (Figure 3a). Fast acquisition of 2D planar information is possible nowadays with high-speed cameras or optical methods to collect the light signals. However, the capability of fast z-focus translation is still lagging behind, which limits the overall 3D imaging rate. This is especially important in real-world industrial manufacturing applications where there are plenty of photons from reflected or scattered light (i.e. high photon-budget) but the limitation arises from the insufficient z-focus translation speed. Additionally, in the area of microscopy recent improvements in the quantum efficiency of various detectors, the development of brighter dyes and optimized labeling protocols are pushing fluorescence microscopy to high number of photon regimes or

high signal-to-noise ratios (SNR), which in return calls for a development in a faster z-focus control more than ever.

The acquisition of a z-stack over an extended range in a short period of time can be made by implementing a high-speed varifocal lens. Successful examples include the use of an electrically tunable lens for light-sheet fluorescence microscopy (LSFM)[73] (Figure 3b), quantitative phase microscopy[74] and temporal focusing[75], and the use of a TAG lens for bright-field microscopy[63]. In these instances, an image is captured at every pulsed illumination that is synchronized with the variable optical element. Notably, the few or even the lack of mechanical moving parts for focus translation minimizes the waiting time for refocusing to occur enabling rapid acquisition of a z-stack which is now only limited by the camera frame rate or SNR.

Volumetric imaging at faster rates is possible by using an extended DOF (EDOF), as shown in Figure 3c. Although the axial elongation of the focal volume comes at the cost of sacrificing the retrieval of the accurate z-position coordinates of the imaged elements, EDOF has still been proven to be advantageous for fast characterization of sparse events, such as neuronal transients[76], or the topography of microstructures[77]. In comparison to traditional methods such as phase masks or axicons to generate a Bessel beam, high-speed varifocal elements can be used to create a dynamic EDOF with a tunable axial range[43,78–80]. Dynamic EDOF can help achieve axial-invariance in the point-spread function (PSF)[81] which aids in full recovery of 3D image sharpness by using easier-to-implement 2D deconvolution algorithms[43,78]. To obtain a dynamic EDOF, an unsynchronized z-focus sweep that is faster than the exposure time of the detector is the key. The exposure time is typically in the order of milliseconds for wide-field systems but can go down to tens of microseconds in point-scanning systems. Therefore for dynamic EDOF generation, while relatively slow varifocal elements can be used in wide-field architectures, ultra-high speed varifocal elements are essential in point-scanning systems such as confocal and two-photon microscopy[79,80] Examples of EDOF volumetric imaging are presented in Figures 3d and 3e.

As a matter of fact, the fastest 3D imaging can be accomplished by acquiring an entire z-stack simultaneously, as illustrated in Figure 3f. This can be accomplished by using light-field systems that capture information of both intensity and direction of light. However they are only compatible with wide-field systems and normally come at the cost of a loss in spatial resolution[82,83]. Variable optical elements can be a good alternative approach that allows quasi-simultaneous imaging of two or more focal planes when used with synchronized illumination or detection. By using pulsed illumination synchronized with a varifocal lens, biplane imaging has been implemented for wide-field systems. When combined with color or time encoding, information from the two planes acquired in single or consecutive frames was extracted in a post-processing step[84,85]. In another example of confocal[72,86] and two-photon[59,79,87,88] microscopes, pixel-by-pixel multiplane capture has been made possible with an ultra-high-speed liquid lens and synchronized detection. In this case, the high z-focus translation allowed one or multiple axial scans to be performed during the pixel dwell time. The detection of the arrival time of the photons using fast readout electronics with sub-microsecond timing accuracy allows sorting the photons into a user-defined number of planes, producing high intravital imaging speeds (Figure 3g-h).

On a last note, the trade-off between the 3D imaging speed and an acceptable SNR will always exist and therefore continuous efforts are being made to address this issue; besides the continuous improvement in detectors and fluorescent labels, the seamless integration of hardware and software into modular systems has recently shown promise to capture image volumes at unprecedented rates[89,90].

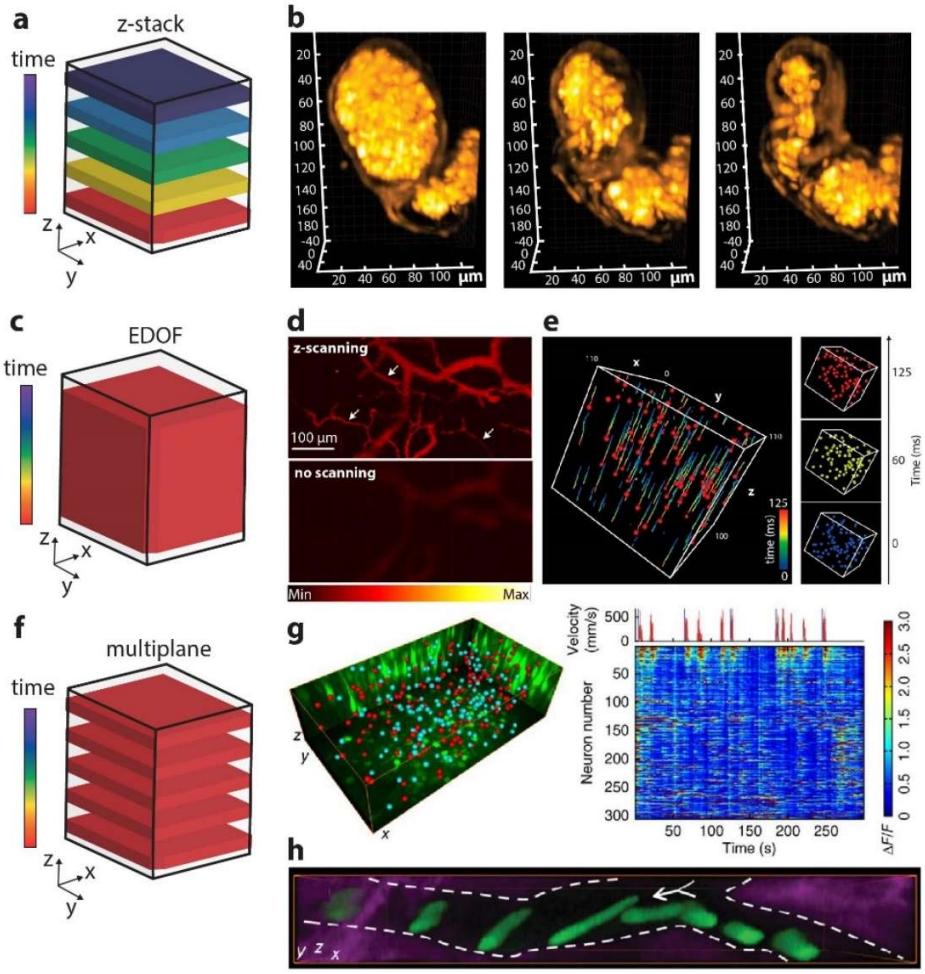

Figure 3. Examples of volumetric imaging using variable optical elements. *(a) Normal mode of 3D acquisition by capturing of a z-stack. (b) Time sequence of 3 reconstructed volumes of a beating Zebrafish heart obtained with light-sheet fluorescence microscopy. Adapted from Ref* [73]*. (c) Extended depth of field (EDOF) method to acquire volumetric data.(d) Normalized photoacoustic images of a mouse ear with fast z-scanning (top) and no scanning (bottom). Adapted from Ref* [91]*. (e) Imaging of flowing beads captured with a light-sheet microscope with an unsynchronized TAG lens in the detection arm. From Ref* [92] *(f) Fast volumetric imaging by simultaneous capturing of multiple planes. (g) Representative volume view (left) and corresponding calcium dynamics (right) of neuronal events from a behaving mouse with a two-photon microscope and a TAG lens. From Ref* [59] *(h) Snapshots of a neutrophil flowing through a vascular junction, same system as in e. From Ref* [88]*.*

Increased statistics and data acquisition speed. The demand for optical techniques capable of extracting quantitative data is continuously growing. One example is single molecule localization techniques[93], which are not only capable of attaining images with enhanced spatial detail but also of quantifying the number of fluorophores or even molecules. Other optical techniques such as single particle tracking[94] (SPT) or FCS[95] are routinely used to quantify velocity, diffusion coefficient and other important parameters of targeted specimens that can lead to the unmasking of the dynamics of key processes including virus trafficking or molecular diffusion at synapses. In these cases, fast variable optical elements can improve the quality of the data acquired and reduce the uncertainty of the measured parameters. For example, the use of a high-speed varifocal lens for SPT facilitated the gathering of information from different focal planes and enabled tracking of multiple micro and nanoscale objects over an axial range which have not

possible with the traditional systems[96,97]. Figures 4(a)-(b) show 3D trajectories of a freely diffusing virus-like particle[98] and 1-µm beads[96] which was then used to study the extracellular behavior of single virons, and to track the movement in an evaporating drop of a water. Similarly, an optical feedback SPT system featuring a TAG lens provided real-time 3D-tracking of fluorescent nanoparticles and quantum dots with high speed and high-localization precision using relatively low photon numbers[98]. The increased statistics collected with variable optical elements has also been shown to have a positive impact in techniques that rely on correlative data fluctuations, such as FCS[62] mentioned in the previous section. In this case, the timely collection of data from multiple axial positions offers two advantages. First, a gain in the accuracy of the measured parameters. Second, the possibility to perform additional correlation analysis along different axial data points and unveil asymmetric dynamics. Importantly, the growing number of novel super-resolution fluorescence microscopies based on fluctuation analysis[99–101] could also benefit from the increased amount of information collected through fast variable optical elements. Since the quality of the reconstructed images depends on the number of collected frames, increased data acquisition speed can lead to better-resolved images.

Another example where increase in statistics and data acquisition speed can benefit is for ultra-fast manufacturing applications. In industrial settings, the capability to rapidly prototype and perform complex metrological analysis is indispensable to maintain a high-quality controlled process. One of the challenges associated with dimensional metrology is to generate highly accurate 3D relative motions between sensors and measured surfaces with sub-µm resolutions. An ultra-high-speed varifocal lens has been implemented to develop a highly accurate confocal point sensor for nano- coordinate measuring systems (CMS)[102]. Combined with a signal processing method, light-information from the fast focus modulation has been used in the confocal point sensor to significantly improve accuracy and to reduce measurement uncertainty and the probing time. For real-world industrial applications, an ultra-high-speed varifocal lens was used in a wide-field system to provide sufficient number of image-data frames at a rapid rate in order to analyze samples with a height that is orders of magnitude larger than that of the biological or lab-scale samples[63]. Figures in 4(c) show a metrological analysis example of a tooth-brush head, a general consumer product, and the positions of 54 image focal-planes that were collected over a 9-mm height. Aided by a post computational process, a quantitative data-set on the brush height and angles was acquired. Thus, the high-resolution and high-speed data acquisition enabled by an ultra-high-speed varifocal lens allows a detailed metrological analysis that can help with the rapid prototyping and quality control process for industrial applications.

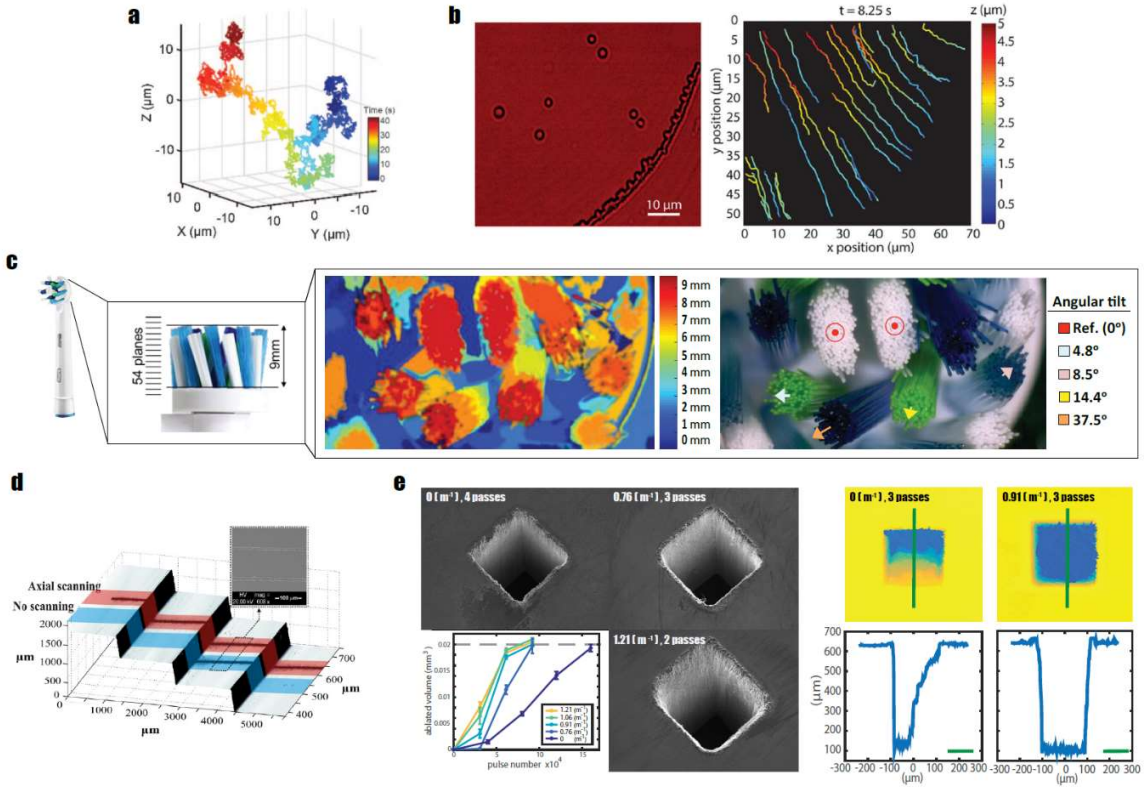

Figure 4. Examples of retrieving enhanced quantitative data and laser micromachining via varifocal optics. *(a) 3D trajectory of single fluorescent bead in water.* [98]*, (b) 3D tracking of beads in an evaporating water droplet. Snapshot of the beads at 8.25 s and their particle-trajectory color-plot.*[96]*, (c) Oral-B electronic tooth-brush used for analysis, relative height analysis and relative angular measurements of the bristles.* [63]*. (d) Line machining silicon on stepped surfaces with axial scanning on vs. off. All 4 surfaces are micromachined with axial scanning.* [64]*. (e) (left) SEM images of square holes ablated without a z-scanner (0 m^{-1} lens power (LP)) with 4 passes, 3 passes with scanning (0.76m^{-1} varifocal LP) and 2 passes with scanning (1.21m^{-1} varifocal LP). Measured ablated volume vs. pulse number shown in plot* [65]*. (right) Vertical cross-sectional profiles of the ablated squares with no focus modulation vs 3 passes with 0.91 m^{-1} varifocal LP*[65]*.*

Enhanced temporal and spatial control over 3D beam focus. In general, tightly focused beams are desired for various applications such as high-resolution imaging, optical trapping, 3D printing, laser machining, and optical communications. However, tight-focusing of the laser beam into micrometer-sized spots inevitably results in a shallow DOF along the axial direction. Especially for laser printing and machining applications, shallow DOF prevents laser processing of uneven surfaces with height differences larger than the DOF and entails refocusing of the sample surface by translating the sample-holding stage for every step. Implementation of varifocal optical elements obviates the need for exact surface profiling and re-adjustment of the focus every time. The faster the focus is modulated, the higher the laser processing rate can be achieved. In addition, when combined with the capability to micromachine on the μs time scale at which heat dissipation occurs, laser-processing with high-speed varifocal optics can considerably increase the efficiency in various micromachining applications. Figures 4(d) and 4(e) show examples of using an ultra-high-speed varifocal lens to enhance temporal and spatial control over 3D beam focus for high throughput, high-precision laser micromachining. In figure 4(d), lines are micromachined on a stack of 4 silicon wafers. When an ultra-high-speed variable focal lens inserted, it has been shown that lines can be

written on each of all 4 uneven silicon surfaces for a total scanning range that is as twice as deep when compared with those written with no focus modulation. Figure 4(e) demonstrates higher throughput laser micromachining of silicon wafers achieved by using an ultra-high-speed varifocal lens. On the left, SEM images of three 200-µm by 200-µm, 500-µm depth square ablated holes are compared, each with and without a varifocal lens with varying number of laser passes. While only 2 passes are required to ablate the square hole with a varying focal lens, a total of 4 passes are required to ablate the same amount of volume without any focus modulation. Figures on the right show a comparison of vertical cross-sectional profiles of two holes, each written with no focus modulation and with a varying focal lens operation. The increased micromachining rate demonstrated in these figures leads to realization of higher-throughput micromachining for future industrial applications.

Conclusions and outlook

The capability to precisely vary focus at ultra-high-speeds opens the door to new applications in 3D biomedical imaging, industrial inspection, spectroscopies, and other optical characterization and materials modifications methods. Continuous progress in the speed and quantum efficiency of optical detectors, together with faster electronics, makes implementation of variable optical elements into traditional systems easier than ever. For imaging in general, fast axial focus control of light entails rapid acquisition of sufficient image-data over an extended depth which enables real-time volumetric imaging. For bio-samples, fast focus modulation prevents photobleaching and phototoxicity effects for increased efficiency. In laser processing applications, adapting fast focal varying lenses into the system enhances the depth of field which removes the need for z-focus control during processing without lateral resolution loss. Hence, the enhancement in temporal and spatial control enables not only more efficient imaging and spectroscopies for lab-scale applications but also higher-throughput for industrial inspection and manufacturing areas.

We expect the technological impact of the development towards higher-speed varifocal optical elements will go beyond the few examples we have reviewed in this article. For example, miniaturization of the ultra-high-speed varifocal optics combined with optofluidics research can help achieve ultra-high-speed optical communications. As new material properties get discovered and innovative light manipulating principles get implemented to enhance the focal-varying response, interesting applications will continue to emerge to advance both the scientific and industrial communities.

Acknowledgements

The authors acknowledge financial support from Princeton University. MD is a Serra Hunter Fellow. MD acknowledges Compagnia di San Paolo, ROL 34704.

References

1. Bawart, M., Jesacher, A., Zelger, P., Bernet, S. & Ritsch-Marte, M. Modified Alvarez lens for high-speed focusing. *Opt. Express* **25**, 29847–29855 (2017).

2. Radhakrishnan, H. & Charman, W. N. Optical characteristics of Alvarez variable-power spectacles. *Ophthalmic Physiol. Opt.* **37**, 284–296 (2017).

3. Zou, Y., Zhang, W., Tian, F., Siong Chau, F. & Zhou, G. Development of miniature tunable multi-element Alvarez lenses. *IEEE J. Sel. Top. Quantum Electron.* **21**, 2–9 (2015).

4. Bernet, S., Harm, W. & Ritsch-marte, M. Demonstration of focus-tunable diffractive Moir´e-lenses. *Opt. Express* **21**, 4317–4322 (2013).

5. Mishra, K., van den Ende, D. & Mugele, F. Recent developments in optofluidic lens technology. *Micromachines* **7**, (2016).

6. Choi, J. M., Son, H. M. & Lee, Y. J. Biomimetic variable-focus lens system controlled by winding-type SMA actuator. *Opt. Express* **17**, 8152–8164 (2009).

7. Fuh, Y. K., Huang, W. C., Lee, Y. S. & Lee, S. An oscillation-free actuation of fluidic lens for optical beam control. *Appl. Phys. Lett.* **101**, 2010–2013 (2012).

8. Hasan, N., Kim, H. & Mastrangelo, C. H. Large aperture tunable-focus liquid lens using shape memory alloy spring. *Opt. Express* **24**, 13334 (2016).

9. Kim, J., Lee, J. & Won, Y. H. Method to reduce the aberration of a polygonal aperture focus-tunable lens array for high fill factor. *Opt. Lett.* **44**, 2554 (2019).

10. Cao, J. *et al.* Bioinspired Zoom Compound Eyes Enable Variable-Focus Imaging. *ACS Appl. Mater. Interfaces* **12**, 10107–10117 (2020).

11. Ee, H. S. & Agarwal, R. Tunable Metasurface and Flat Optical Zoom Lens on a Stretchable Substrate. *Nano Lett.* **16**, 2818–2823 (2016).

12. She, A., Zhang, S., Shian, S., Clarke, D. R. & Capasso, F. Adaptive metalenses with simultaneous electrical control of focal length, astigmatism, and shift. *Sci. Adv.* **4**, 1–8 (2018).

13. Aiello, M. D. *et al.* Achromatic Varifocal Metalens for the Visible Spectrum. *ACS Photonics* **6**, 2432–2440 (2019).

14. Ren, H., Xianyu, H., Xu, S. & Wu, S.-T. Adaptive dielectric liquid lens. *Opt. Express* **16**, 14954–14960 (2008).

15. Lu, Y. S., Tu, H., Xu, Y. & Jiang, H. Tunable dielectric liquid lens on flexible substrate. *Appl. Phys. Lett.* **103**, (2013).

16. Jin, B., Ren, H. & Choi, W.-K. Dielectric liquid lens with chevron-patterned electrode. *Opt. Express* **25**, 32411–32419 (2017).

17. Miccio, L., Paturzo, M., Grilli, S., Vespini, V. & Ferraro, P. Hemicylindrical and toroidal liquid microlens formed by pyro-electro-wetting. *Opt. Lett.* **34**, 1075–1077 (2009).

18. Hao, C. *et al.* Electrowetting on liquid-infused film (EWOLF): Complete reversibility and controlled droplet oscillation suppression for fast optical imaging. *Sci. Rep.* **4**, 1–7 (2014).

19. Li, L., Wang, J.-H., Wang, Q.-H. & Wu, S.-T. Displaceable and focus-tunable electrowetting optofluidic lens. *Opt. Express* **26**, 25839 (2018).

20. Lee, J., Park, Y. & Chung, S. K. Multifunctional liquid lens for variable focus and aperture. *Sensors Actuators A Phys.* **287**, 177–184 (2019).

21. Shin, D., Kim, C., Koo, G. & Won, Y. Depth plane adaptive integral imaging system using a vari-focal liquid lens array for realizing augmented reality. *Opt. Express* **28**, 5602–5616 (2020).

22. Xiao, W. & Hardt, S. An adaptive liquid microlens driven by a ferrofluidic transducer. *J. Micromechanics Microengineering* **20**, (2010).

23. Cheng, H. C., Xu, S., Liu, Y., Levi, S. & Wu, S. T. Adaptive mechanical-wetting lens actuated by ferrofluids. *Opt. Commun.* **284**, 2118–2121 (2011).

24. Oku, H. & Ishikawa, M. High-speed liquid lens with 2ms response and 80.3 nm root-mean-square wavefront error. *Appl. Phys. Lett.* **94**, 2–5 (2009).

25. Patra, R., Agarwal, S., Kondaraju, S. & Bahga, S. S. Membrane-less variable focus liquid lens with manual actuation. *Opt. Commun.* **389**, 74–78 (2017).

26. Dong, L., Agarwal, A. K., Beebe, D. J. & Jiang, H. Adaptive liquid microlenses activated by stimuli-responsive hydrogels. *Nature* **442**, 551–554 (2006).

27. Kim, J., Kim, J., Na, J.-H., Lee, B. & Lee, S.-D. Liquid crystal-based square lens array with tunable focal length. *Opt. Express* **22**, 3316 (2014).

28. Zhou, Z., Li, X. & Ren, H. Liquid crystal lens with a concave polyimide layer. *Opt. Eng.* **56**, 077102 (2017).

29. Kim, S. U., Na, J. H., Kim, C. & Lee, S. D. Design and fabrication of liquid crystal-based lenses. *Liq. Cryst.* **44**, 2121–2132 (2017).

30. Ma, Y. *et al.* Fast switching ferroelectric liquid crystal Pancharatnam-Berry lens. *Opt. Express* **27**, 10079 (2019).

31. Chen, H. *et al.* A large bistable negative lens by integrating a polarization switch with a passively anisotropic focusing element. **22**, 2045–2052 (2014).

32. Bharath, M. *et al.* Compact vari-focal augmented reality display based on ultrathin , polarization-insensitive , and adaptive liquid crystal lens. *Opt. Lasers Eng.* **128**, 26–32 (2020).

33. Yin, S. *et al.* Nanosecond KTN varifocal lens without electric field induced phase transition. *Photonic Fiber Cryst. Devices Adv. Mater. Innov. Device Appl. XI* 27 (2017) doi:10.1117/12.2276511.

34. Sohan Kawamura, Tadayuki Imai, Jun Miyazu, Tadashi Sakamoto, and J. K. 2 . 5-fold increase in lens power of a KTN varifocal lens by employing an octagonal structure. *Appl. Opt.* **54**, (2015).

35. Inagaki, T., Imai, T., Miyazu, J. & Kobayashi, J. Polarization independent varifocal lens using KTN crystals. *Opt. Lett.* **38**, 2673 (2013).

36. Shibaguchi, T. & Funato, H. Lead-lanthanum zirconate-titanate (Plzt) electrooptic variable focal-length lens with stripe electrodes. *Jpn. J. Appl. Phys.* **31**, 3196–3200 (1992).

37. Mermillod-blondin, A., Mcleod, E. & Arnold, C. B. Acoustic Gradient Index of Refraction Lens. *Opt. Lett.* **33**, 2146–2148 (2008).

38. Koyama, D., Isago, R. & Nakamura, K. Three-dimensional focus scanning by an acoustic variable-focus optical liquid lens. *AIP Conf. Proc.* **1474**, 355–358 (2012).

39. Koyama, D., Isago, R. & Nakamura, K. Ultrasonic variable-focus optical lens using viscoelastic material. *Appl. Phys. Lett.* **100**, (2012).

40. Kaplan, A., Friedman, N. & Davidson, N. Acousto-optic lens with very fast focus scanning. *Opt. Lett.* **26**, 1078–1080 (2001).

41. Reddy, G. D. & Saggau, P. Fast three-dimensional laser scanning scheme using acousto-optic deflectors. *J. Biomed. Opt.* **10**, 064038 (2005).

42. Boucher, P., Barré, N., Pinel, O., Labroille, G. & Treps, N. Continuous axial scanning of a Gaussian beam via beam steering. *Opt. Express* **25**, 23060 (2017).

43. Shain, W. J., Vickers, N. A., Goldberg, B. B., Bifano, T. & Mertz, J. Extended depth-of-field microscopy with a high-speed deformable mirror. *Opt. Lett.* **42**, 995–998 (2017).

44. Žurauskas, M., Barnstedt, O., Frade-Rodriguez, M., Waddell, S. & Booth, M. J. Rapid adaptive remote focusing microscope for sensing of volumetric neural activity. *Biomed. Opt. Express* **8**, 4369 (2017).

45. Salter, P. S., Iqbal, Z. & Booth, M. J. Analysis of the Three-Dimensional Focal Positioning Capability of Adaptive Optic Elements. *Int. J. Optomechatronics* **7**, 1–14 (2013).

46. Duocastella, M. & Arnold, C. B. Transient response in ultra-high speed liquid lenses. *J. Phys. D. Appl. Phys.* **46**, 075102 (2013).

47. Sato, S. Applications of liquid crystals to variable-focusing lenses. *Opt. Rev.* **6**, 471–485 (1999).

48. Lin, Y., Wang, Y. & Reshetnyak, V. Liquid crystal lenses with tunable focal length. *Liq. Cryst. Rev.* **5**, 111–143 (2017).

49. Lin, Y., Wang, Y. & Reshetnyak, V. Liquid crystal lenses with tunable focal length. *Liq. Cryst. Rev.* **5**, 111–143 (2017).

50. Rahman, A., Said, S. M. & Balamurugan, S. Blue phase liquid crystal : strategies for phase stabilization and device development. doi:10.1088/1468-6996/16/3/033501.

51. Xu, S. *et al.* Fast-Response Liquid Crystal Microlens. *Micromachines* **5**, 300–324 (2014).

52. Guo, Q., Zhao, X., Zhao, H. & Chigrinov, V. G. Reverse bistable effect in ferroelectric liquid crystal devices with ultra-fast switching at low driving voltage. *Opt. Lett.* **40**, 2413–2416 (2015).

53. Sreenilayam, S. P. *et al.* Spontaneous helix formation in non-chiral bent-core liquid crystals with fast linear electro-optic effect. *Nat. Commun.* **7**, 11369 (2016).

54. Basu, R. Effects of graphene on electro-optic switching and spontaneous polarization of a ferroelectric liquid crystal. *Appl. Phys. Lett.* **112905**, (2014).

55. Shukla, R. K. *et al.* Electro-optic and dielectric properties of a ferroelectric liquid crystal doped with chemically and thermally stable emissive carbon dots. *RSC Adv.* **5**, 34491–34496 (2015).

56. Chang, C., Lin, Y., Srivastava, A. K. & Chigrinov, V. G. An optical system via liquid crystal photonic devices for photobiomodulation. *Sci. Rep.* **8**, 4251 (2018).

57. Zhang, Z., You, Z. & Chu, D. Fundamentals of phase-only liquid crystal on silicon (LCOS) devices. *Light Sci. Appl.* **3**, 1–10 (2014).

58. Karagyozov, D., Skanata, M. M., Lesar, A. & Gershow, M. Recording neural activity in unrestrained animals with 3D tracking two photon microscopy. *bioRxiv* 213942 (2017) doi:10.1101/213942.

59. Kong, L. *et al.* Continuous volumetric imaging via an optical phase-locked ultrasound lens. *Nat. Methods* **12**, (2015).

60. Zong, W. *et al.* Large-field high-resolution two-photon digital scanned light-sheet microscopy. *Cell Res.* **25**, 254–257 (2015).

61. Grulkowski, I., Szulzycki, K. & Wojtkowski, M. Microscopic OCT imaging with focus extension by ultrahigh-speed acousto-optic tunable lens and stroboscopic illumination. *Opt. Express* **22**, 31746 (2014).

62. Wei, M. T. *et al.* Phase behaviour of disordered proteins underlying low density and high permeability of liquid organelles. *Nat. Chem.* **9**, (2017).

63. Kang, S., Dotsenko, E., Amrhein, D., Theriault, C. & Arnold, C. B. Ultra-high-speed variable focus optics for novel applications in advanced imaging. in *Proceedings of SPIE - The International Society for Optical Engineering* vol. 10539 (2018).

64. Duocastella, M. & Arnold, C. B. Enhanced depth of field laser processing using an ultra-high-speed axial scanner. *Appl. Phys. Lett.* **102**, 061113 (2013).

65. Chen, T., Fardel, R. & Arnold, C. B. Ultrafast z-scanning for high-efficiency micro-machining. *Light Sci. Appl.* **7**, 17181 (2018).

66. Lopez, C. A. & Hirsa, A. H. Fast focusing using a pinned-contact oscillating liquid lens. *Nat. Photon.* **2**, 610–613 (2008).

67. Murade, C. U., Ende, D. Van Der & Mugele, F. High speed adaptive liquid microlens array. *Opt. Express* **20**, 18180–18187 (2012).

68. Laissue, P. P., Alghamdi, R. A., Tomancak, P., Reynaud, E. G. & Shroff, H. Assessing phototoxicity in live fluorescence imaging. *Nat. Methods* **14**, 657–661 (2017).

69. Icha, J., Weber, M., Waters, J. C. & Norden, C. Phototoxicity in live fluorescence microscopy, and how to avoid it. *BioEssays* **39**, 1–15 (2017).

70. Power, R. M. & Huisken, J. Adaptable, illumination patterning light sheet microscopy. *Sci. Rep.* **8**, 1–11 (2018).

71. Donnert, G., Eggeling, C. & Hell, S. W. Major signal increase in fluorescence microscopy through dark-state relaxation. *Nat. Methods* **4**, 81–86 (2007).

72. Duocastella, M., Vicidomini, G. & Diaspro, A. Simultaneous multiplane confocal microscopy using acoustic tunable lenses. *Opt. Express* **22**, 19293 (2014).

73. Fahrbach, F. O., Voigt, F. F., Schmid, B., Helmchen, F. & Huisken, J. Rapid 3D light-sheet microscopy with a tunable lens. *Opt. Express* **21**, 21010–26 (2013).

74. Zuo, C., Chen, Q., Qu, W. & Asundi, A. High-speed transport-of-intensity phase microscopy with an electrically tunable lens. *Opt. Express* **21**, 24060 (2013).

75. Jiang, J. *et al.* Fast 3-D temporal focusing microscopy using an electrically tunable lens. *Opt. Express* **23**, 24362 (2015).

76. Lu, R. *et al.* Video-rate volumetric functional imaging of the brain at synaptic resolution. *Nat. Neurosci.* **20**, 620–628 (2017).

77. Colomb, T. *et al.* Extended depth-of-focus by digital holographic microscopy. *Opt. Lett.* **35**, 1840–1842 (2010).

78. Liu, S. & Hua, H. Extended depth-of-field microscopic imaging with a variable focus microscope objective. *Opt. Express* **19**, 353–62 (2011).

79. Piazza, S., Bianchini, P., Sheppard, C., Diaspro, A. & Duocastella, M. Enhanced volumetric imaging in 2-photon microscopy via acoustic lens beam shaping. *J. Biophotonics* **11**, e201700050 (2018).

80. Zheng, J., Zuo, C., Gao, P. & Nienhaus, G. U. Dual-mode phase and fluorescence imaging with a confocal laser scanning microscope. *Opt. Lett.* **43**, 5689 (2018).

81. Lu, S.-H. & Hua, H. Imaging properties of extended depth of field microscopy through single-shot focus scanning. *Opt. Express* **23**, 10714 (2015).

82. Prevedel, R. *et al.* Simultaneous whole-animal 3D imaging of neuronal activity using light-field microscopy. *Nat. Methods* **11**, 727–30 (2014).

83. Martínez-Corral, M. & Javidi, B. Fundamentals of 3D imaging and displays: a tutorial on integral imaging, light-field, and plenoptic systems. *Adv. Opt. Photonics* **10**, 512 (2018).

84. Grewe, B. F., Voigt, F. F., van 't Hoff, M. & Helmchen, F. Fast two-layer two-photon imaging of neuronal cell populations using an electrically tunable lens. *Biomed. Opt. Express* **2**, 2035–46 (2011).

85. Sheffield, M. E. J. & Dombeck, D. A. Calcium transient prevalence across the dendritic

arbour predicts place field properties. *Nature* **517**, 200–204 (2015).

86. Szulzycki, K., Savaryn, V. & Grulkowski, I. Rapid acousto-optic focus tuning for improvement of imaging performance in confocal microscopy. *Appl. Opt.* **57**, C14–C18 (2018).

87. Kong, L., Tang, J. & Cui, M. In vivo volumetric imaging of biological dynamics in deep tissue via wavefront engineering. *Opt. Express* **24**, 1214–1221 (2016).

88. Kong, L., Tang, J. & Cui, M. Multicolor multiphoton in vivo imaging flow cytometry. *Opt. Express* **24**, 6126–6135 (2016).

89. Har-gil, H. *et al.* PySight : plug and play photon counting for fast intravital microscopy. *Optica* **5**, 29–37 (2018).

90. Yamato, K., Yamashita, T., Chiba, H. & Oku, H. Fast volumetric feedback under microscope by temporally coded exposure camera. *Sensors* **19**, (2019).

91. Yang, X., Song, X., Jiang, B. & Luo, Q. Multifocus optical-resolution photoacoustic microscope using ultrafast axial scanning of single laser pulse. *Opt. Express* **25**, 28192 (2017).

92. Duocastella, M. *et al.* Fast Inertia-Free Volumetric Light-Sheet Microscope. *ACS Photonics* **4**, 1797–1804 (2017).

93. Deschout, H. *et al.* Precisely and accurately localizing single emitters in fluorescence microscopy. *Nat. Methods* **11**, 253–266 (2014).

94. Manzo, C. & Garcia-parajo, M. F. A review of progress in single particle tracking : from methods to biophysical insights. *Reports Prog. Phys.* **78**, 124601 (2015).

95. Elson, E. L. Fluorescence Correlation Spectroscopy : Past , Present , Future. *Biophys. J.* **101**, 2855–2870 (2011).

96. Duocastella, M., Theriault, C. & Arnold, C. B. Three-dimensional particle tracking via tunable color-encoded multiplexing. *Opt. Lett.* **41**, 863–866 (2016).

97. Sancataldo, G. *et al.* Three-dimensional multiple-particle tracking with nanometric precision over tunable axial ranges. *Optica* **4**, 367 (2017).

98. Hou, S., Lang, X. & Welsher, K. Robust real-time 3D single-particle tracking using a dynamically moving laser spot. *Opt. Lett.* **42**, 2390 (2017).

99. Dertinger, T., Colyer, R., Iyer, G., Weiss, S. & Enderlein, J. Fast, background-free, 3D super-resolution optical fluctuation imaging (SOFI). *Proc. Natl. Acad. Sci.* **106**, 22287–22292 (2009).

100. Agarwal, K. & Macha, R. Multiple signal classification algorithm for super-resolution fluorescence microscopy. *Nat. Commun.* **7**, 13752 (2016).

101. Ashdown, G., Owen, D. M., Pereira, P. M., Gustafsson, N. & Henriques, R. Fast live-cell

conventional fluorophore nanoscopy with ImageJ through super-resolution radial fluctuation. *Nat. Commun.* **7**, 1–9 (2016).

102. Hausotte, T., Gröschl, A. & Schaude, J. High-speed focal-distance-modulated fiber-coupled confocal sensor for coordinate measuring systems. *Appl. Opt.* **57**, 3907 (2018).

103. Sancataldo, G. *et al.* Three-dimensional multiple-particle tracking with nanometric precision over tunable axial ranges. *Optica* **4**, 367 (2017).

104. Sheppard, C. J. R. Limitations of the paraxial Debye approximation. *Opt. Lett.* **38**, 1074–1076 (2013).